

*Article*

## 200W PEM Fuel Cell Stack with Online Model-Based Monitoring System

Pittaya Khanungkhid<sup>1</sup> and Pornpote Piumsomboon<sup>1,2,\*</sup>

<sup>1</sup> Fuels Research Center, Department of Chemical Technology, Faculty of Science, Chulalongkorn University, 254 Phayathai Road, Patumwan, Bangkok 10330, Thailand

<sup>2</sup> Center of Excellence on Petrochemical and Materials Technology, Chulalongkorn University, 254, Phayathai Road, Patumwan, Bangkok 10330, Thailand

\*E-mail: pornpote.p@chula.ac.th

**Abstract.** Although various designs have been introduced to improve the performance of a Proton Exchange Membrane Fuel Cell (PEMFC) stack system, fault conditions, such as drying or flooding, may still occur due to the complexity of the process. The development of a system which can detect these fault conditions is a key to operate PEMFC stack system effectively. In this study, a monitoring system for a 200W commercial PEMFC stack system has been developed by constructing models for determining the flooding and drying conditions inside the cell. Since the membrane resistance and pressure drop across the stack are important parameters for determining either drying or flooding conditions taking place inside the fuel cell, the online model-based monitoring system is developed by adopting existing algorithms. A number of instruments are installed to measure relevant data. The data acquisition system and mathematical models have been programmed under LabVIEW™ environment. To indicate the abnormal conditions inside the fuel cell stack, the model prediction is compared with the experimental measured values and the size of the discrepancy will be an indicator.

**Keywords:** Fuel cell, PEM, monitoring, model-based.

ENGINEERING JOURNAL Volume 18 Issue 4

Received 17 February 2014

Accepted 11 June 2014

Published 16 October 2014

Online at <http://www.engj.org/>

DOI:10.4186/ej.2014.18.4.13

## 1. Introduction

Fuel cells are energy conversion devices which directly convert the chemical energy of fuel into electrical energy. The use of fuel cells offers advantages for many applications, such as zero emission, high energy density, and improving efficiency. They are the candidates for an efficient and clean power source to supply the need of power in the future. Proton Exchange Membrane (PEM) fuel cells are expected to play an important role, where they will be used in both portable and stationary applications. PEM fuel cells have some unique features when compared to other types of fuel cells, such as low operating temperature, relative simplicity of their designs, less noise, and high energy density [1, 2].

In a PEM fuel cell, hydrogen and oxygen react, producing water, heat, and electricity. Water is typically introduced to both anode and cathode channels. At the cathode, water is produced by oxygen reduction reaction, and is additionally forced by electro-osmotic drag from the anode side. On the contrary, water can also be pushed from the cathode side to the anode side by back-diffusion. Moreover, additional liquid water is formed on both sides by the effect of condensation. The accumulation of water inside the cells is a major consideration in the operation of a PEM fuel cell. This accumulated water reduces the path available for the transport of oxygen to reach the reaction sites, resulting in the drop of its performance. This phenomenon is called cell flooding. On the other hand, if the water is not enough in the system by the heat within the cell stacks, the membrane will be dehydrated and its resistance will increase dramatically, causing voltage drop. This phenomenon is called cell drying.

When cells are flooding or drying, the phenomena affected system variables such as cell resistances, cell voltage, friction loss in gas flow channel and subsequently, the cell performance. Thus if these variables have been tracked and measured, their values can imply the condition inside the fuel cell. There are a number of studies being proposed in order to develop monitoring and diagnostic systems. Barbir et al. [3] demonstrated that pressure drop and cell resistance could be effective indicators for identifying flooding and drying, respectively. They performed the experiment on three-cell with 65 cm<sup>2</sup> active area fuel cell stack. The responses of pressure drop and cell resistance were plotted for various operating conditions. Pei et al. [4] also showed that the pressure drop on the hydrogen side of a 10 kW fuel cell stack can be estimated correctly by calculating the friction loss in the flow channel. Stumper et al. [5] presented a diagnostic tool that provides insight about the liquid water distribution in a single custom-design PEM fuel cell using current measurement along the length of the cell. By fitting the experimental data to a simplified Srinivasan equation [6], the pure ohmic resistance of the cell was determined. Later on, Görgün et al. [7] proposed an algorithm for estimating water content in the membrane of a single 50 cm<sup>2</sup> PEM fuel cell. Since water content in the membrane is directly related to membrane resistance, which can be determined from the ohmic loss. The ohmic loss can be estimated from operating parameters, such as voltage, current, pressure and cell temperature. Ma et al. [8] developed diagnostic tool to monitor the water droplet buildup in the transparent single cell PEM fuel cell. The pressure drop between the inlet and outlet of the straight gas channel was studied and the correlation between pressure drop and water removal was developed. Liu et al. [9] studies the characteristics of pressure drop in flow channel with the water flooding. A transparent 5 cm<sup>2</sup> single parallel-flow pattern fuel cell was employed to conduct the experiment. They concluded that the total pressure drop in the flow channel affected by the water resistance to the gas flow. The pressure drop decreases when the cell temperature increases. Chen et al. [10] proposed the use of fast Fourier transform to characterize the relationship between pressure drop and water behavior in each electrode. Roy et al. [11] analyzed flooding in a PEM fuel cells by impedance techniques. They observed that the impedance spectroscopy coupled with a measurement-model-based error analysis can be exploited to identify flooding and drying for PEM fuel cells. Danzer et al. [12] presented the electrochemical parameter identification (EPI) for the characterization of the fuel cell impedances. This method works in the time-domain, resulting in the advantages in comparison with electrochemical impedance spectroscopy, which decreases measurement time and also works with cheaper and simpler hardware.

As being discussed in the previous section, operating variables can indicate the anomaly condition inside fuel cells. A number of studies were conducted by developing models for predicting the observed conditions. Fouquet et al. [13] presented a model-based approach coupled with electrochemical impedance spectroscopy measurement. The results showed the reliable state-of-health monitoring for PEM fuel cells using the membrane resistance, the polarization resistance and the diffusion resistance. Xue et al. [14] proposed a model-based monitoring system using the Hotelling  $T^2$  statistical analysis for PEM fuel cell fault detection. The basic idea is to compare the fuel cell voltage prediction with the fuel cell voltage measurement. Their simulation was conducted by generating measured data from developed model with

including system uncertainties to imitate the actual data. A graphical-probabilistic structure was also proposed for construction a fault diagnosis in PEM fuel cells. Riascos et al. [15] developed the on-line fault diagnosis by applying Bayesian networks. The diagnosis considered 4 types of faults: fault in the air blower, fault in the refrigeration system, growth of fuel crossover and internal loss current, and fault in hydrogen pressure. Mulder et al. [16] presented cell voltage monitoring for PEM fuel cells. Because a drop in cell voltage is caused by many failure situations, the cell voltage monitoring is applicable diagnostic method. They also compared the cell voltage monitor with the laboratory device so that the precision of monitoring was determined. Because of short computing time and easy to implementation, 1-dimensional models have been used to investigate the phenomena in the fuel cells. Gerteisen et al. [17] investigated the phenomena of pore flooding and membrane dehydration of PEM fuel cell with a developed 1-dimensional transient model. Mugikura et al. [18] developed more accurate polarization model and suggested that PEM fuel cell performance degradation is also due to voltage drop by oxygen diffusion and water blocking.

In this paper, an online model-based monitoring system for a 200W commercial PEM fuel cell stack was designed and developed. A number of instrument were installed and transmitted the relevant data reporting the condition of the studied fuel cell, which are stack voltage, load current, stack temperature, hydrogen pressure, and hydrogen pressure drop of a PEM fuel cell, to the data acquisition system. Some of these measurement values were then employed in the mathematical model for predicting related variables under the same operating conditions and brought the prediction values to compare with the experimental measurement. The abnormality, such as flooding or drying, can be indicated from the discrepancy between the model prediction and the measurement values.

## 2. Fuel Cell Model

### 2.1. Electrochemical Reaction

Several mathematical models of a PEM fuel cell were proposed, for example, in the literatures [1, 2, 10-15]. The models of a PEM fuel cell generally consist of thermodynamic model, electrochemistry model, and fluid flow and heat transfer model. The models typically provide the information of fuel cell operation such as the amount of fuel consumption and water generation, cell potential, cell temperature, or pressure drop in the flow channel, etc. These models were adopted for developing the monitoring system in the study.

The Nernst equation [1, 2], which is the function of fuel type and operating condition, was used to estimate the reversible cell voltage,  $E_r$ .

$$E_r = - \left[ \frac{\Delta H}{nF} - \frac{T\Delta S}{nF} \right] + \frac{RT}{nF} \ln \left( \frac{P_{H_2} P_{O_2}^{1/2}}{P_{H_2O}} \right) \quad (1)$$

where  $\Delta H$  and  $\Delta S$  are the enthalpy and entropy changes of the fuel.  $P_{H_2}$ ,  $P_{O_2}$  and  $P_{H_2O}$  are the partial pressures of hydrogen, oxygen and water in the cell.  $R$ ,  $T$ , and  $F$  are the universal gas constant, stack temperature and Faraday's constant, respectively.  $n$  is the number of electrons per molecule of hydrogen. The fuel cell in the study was operated in dead-end mode, the pressure of hydrogen was assumed to be constant. For the cathode side, air was supplied by a blower so the pressure of air is set to be 1 atm. The stack temperature was measured by probing a thermocouple at the cooling air outlet from the stack.

The actual cell voltage decreases from its theoretical value since there are several losses inside the cell. These are the reaction kinetics, the ohmic, and the mass transport losses, as described by Laminie et al. [1]. In general, Eq. (1) can provide the cell voltage of a single cell. When a number of cells are connected in series as a stack, the actual voltage can be calculated by using Eq. (2).

$$V_{st} = N(E_r - V_a - V_{ohm} - V_{conc}) \quad (2)$$

where  $V_{st}$  is stack output voltage,  $N$  is the number of cells connecting in a stack,  $E_r$  is theoretical cell potential,  $V_a$  is the voltage loss due to reaction kinetic,  $V_{ohm}$  and  $V_{conc}$  are those due to the resistances and the mass transport, respectively. These losses could be calculated using the following equations. The reaction kinetic or activation voltage loss and the resistance or ohmic loss are given by empirical formula in Eqs. (3) - (4), respectively.

$$V_a = \frac{RT}{\alpha F} \ln \left( \frac{i}{i_0} \right), \quad (3)$$

$$V_{ohm} = (R_m + r)I \quad (4)$$

where  $\alpha$ , and  $i_0$  are transfer coefficient and exchange current density, respectively. The exchange current density,  $i_0$ , depends on operating conditions and the properties of catalyst, and must be determined experimentally.  $R_m$  and  $r$  are membrane and other component's resistances. The membrane resistance depends on water content in the membrane. The water content,  $\lambda_m$ , is typically defined as the number of water molecules per sulfonic acid groups present in the polymer [2].  $F$ ,  $I$ ,  $R$ , and  $T$  are Faraday constant, electrical current, gas constant, and temperature in Kelvin, respectively. The relationship between membrane resistance and water content was first presented by Springer et al. [19], as described below.

$$R_m = \frac{t_m}{A_m(0.00514\lambda_m - 0.00326)} \exp\left[1268\left(\frac{1}{T} - \frac{1}{303}\right)\right] \quad (5)$$

where  $t_m$  is membrane thickness, and  $A_m$  is membrane active area. Therefore, if the membrane resistance was measured or calculated with given cell temperature, the water content could be evaluated from Eq. (5). In general the cell stack will be run in the region where the ohmic loss is dominant in the potentials loss of the cell and is not run in the region of concentration limitation. Thus, the concentration voltage loss term in Eq. (2) is ignored from the model.

## 2.2. Pressure Drop across the Stack

According to the two-phase separated flow model published in Yu et al. [20], the total pressure drop through the flow field of the fuel cell stack is divided into frictional pressure drop, momentum pressure drop, and gravitational pressure drop, written as Eq. (6).

$$-\left(\frac{dP}{dz}\right)_{total} = -\left(\frac{dP}{dz}\right)_{frictional} - \left(\frac{dP}{dz}\right)_{momentum} - \left(\frac{dP}{dz}\right)_{gravitational} \quad (6)$$

In order to characterize the flooding condition, we assume that the flow inside the flow channel of the fuel cell stack is single-phase flow, so that the flooding condition can be declared if the measured values of pressure drop deviate significantly from its predicted values because of the presence of liquid water in the system. From the model described by Eq. (6), the first term on the right hand side represented the frictional term. The single-phase frictional pressure drop is expressed as a function of the friction coefficient  $C_f$ , written as [11].

$$-\left(\frac{dP}{dz}\right)_{frictional} = \frac{4C_f}{D_e} \frac{G_g^2}{2\rho_g}, \quad (7)$$

$$\Delta P_{frictional} = -\left(\frac{dP}{dz}\right)_{frictional} \times L \quad (8)$$

where  $G_g$  and  $\rho_g$  are the mass flux of gas and gas density, respectively.  $D_e$  is equivalent diameter of the gas flow channel and  $L$  is the effective length of the flow channel. The friction coefficient is a function of surface roughness and Reynolds number ( $Re$ ). For laminar flow, the friction coefficient can be calculated as inverse relation with Reynolds number using Eq. (9) [14]:

$$C_f = \frac{33.8}{Re} \quad (9)$$

To specify the hydrogen input to the fuel cell, the mass flux of hydrogen,  $G_{H_2}$ , is calculated using Faraday's Law:

$$G_{H_2} = \frac{I}{2FA_c} M_{H_2} \quad (10)$$

where  $I$  is current,  $A_c$  is cross-sectional area of the channel,  $F$  is Faraday number and  $M_{H_2}$  is molecular weight of hydrogen. When the fuel cell is in operation, the hydrogen or fuel is consumed along the flow channel. Therefore, the gas mass flux is the function of the position in the flow channel and it can be calculated using Eq. (11):

$$G_g(Z) = \left(1 - \frac{1}{st} \cdot \frac{Z}{L}\right) G_g \quad (11)$$

where  $Z$  is the distance from the inlet along the flow channel and,  $st$  is the stoichiometric ratio.

The second term on the right hand side of Eq. (6) is the pressure drop relating to the consumption of the reactants due to the electrochemical reaction taking place during the current being drawn from the fuel cell stack. The pressure drop is called momentum pressure drop. The total momentum pressure drop must be accumulated along the whole channel using Eqs. (12) and (13).

$$-\int_0^L \left( \frac{dP}{dz} \right)_{\text{momentum}} dz = \left[ G_{\text{total}}(z)^2 \left( \frac{x(z)^2}{\alpha_v(z)\rho_g} + \frac{(1-x(z))^2}{(1-\alpha_v(z))\rho_l} \right) \right]_0^L, \quad (12)$$

$$\Delta P_{\text{momentum}} = \left[ G_{\text{total}}(z)^2 \left( \frac{x(z)^2}{\alpha_v(z)\rho_g} + \frac{(1-x(z))^2}{(1-\alpha_v(z))\rho_l} \right) \right]_0^L, \quad (13)$$

$$\alpha_v = \left[ 1 + \left( \frac{u_g}{u_l} \frac{1-x}{x} \frac{\rho_g}{\rho_l} \right) \right]^{-1} \quad (14)$$

where  $G_{\text{total}}$  and  $\rho_l$  are the mass flux of total gas and liquid density, respectively.  $x$  is mass fraction of gas in the flow field and  $\alpha_v$  represents the void fraction in the gas channel.  $u_g$  and  $u_l$  are velocities of gas and liquid phases, respectively.

The third term on the right hand side of Eq. (6) is the gravitational pressure drop and could be calculated as Eq. (15).

$$-\left( \frac{dP}{dz} \right)_{\text{gravity}} = g [\alpha_v \rho_g + (1-\alpha_v) \rho_l] \sin \theta \quad (15)$$

where  $g$  is the acceleration of gravity and,  $\theta$  is the inclination angle of the flow direction with respect to the horizontal plane.

$$\Delta P_{\text{gravity}} = -\left( \frac{dP}{dz} \right)_{\text{gravity}} \times L \quad (16)$$

According to the above assumption, the gravitational pressure drop can be neglected, since there is no liquid water inside the flow field.

According to Barbir [2], fault detection of a PEM fuel cell can generally be categorized into two types. First, faults that can be directly detected, such as hydrogen leakage. Second, faults that cannot be directly detected such as drying and flooding inside the fuel cell. In order to detect these phenomena, an algorithm for estimating some important parameters corresponding to both phenomena was proposed and developed. The proposed algorithm was programmed and demonstrated with a 200W PEM fuel cell stack.

Using the estimation of membrane water content and pressure drop across the fuel cell stack, the effects of cell drying and cell flooding will be detected during operation of fuel cell stack, respectively. While pressure drop through the channel remains constant with cell drying, its value will be increased with cell flooding [21]. Moreover, the fuel cell will be drying with decreasing of membrane water content below the value of 4 [22]. Below this value, there is not enough water in the cluster around the sulphonate group of the membrane structure. The water content helps facilitating proton mobility in the membrane and leading to high conductivity. According to all above equations, the algorithm for the prediction of the membrane drying-out and flooding condition can be presented in Fig. 1 and 2, respectively.

### 3. Experimental

#### 3.1. Specifications of the Test Equipment

The experimental data was obtained from a 200W PEM fuel cell stack, produced by Horizon Fuel Cell Technologies, as shown in Fig. 3. The system was designed as open-cathode configuration. The stack is composed of 42 cells with 19 cm<sup>2</sup> active area for each cell. On one end, there were two electric fans installed. These fans induce air from the other end of the stack passing through air channels between each cell in order to supply oxygen and remove generating heat from the cell. Figure 4 shows the schematic diagram of the set-up experiment. Hydrogen with 99.99 % purity from a tank was fed in the dead-end mode of operation. The fuel cell system is self-humidified and air-cooled by a small blower, which is also used for supplying air to the cells. A pressure transmitter (ifm model PA3026) and differential pressure

transmitter (Huba control Type 652) were installed for pressure and pressure drop measurements over the range of 0 – 2.5 barg and 0.01 – 0.1 bar, respectively. The pressure transmitter was installed at the inlet side of the fuel cell stack to measure the inlet pressure, while the lines of inlet and outlet reactant gases connecting to the fuel cell stack system were fed to the differential pressure transmitter to measure the pressure drop across the whole fuel cell stack. In addition, stack temperature and humidity of the outlet gas were also measured using thermocouple and humidity transmitter, respectively. The fuel cell was connected with electronic load model N3306A, produced by Agilent Technologies, to vary the current drawn from the system by changing the system potentials. These measurements were then fed into a personal computer (PC) running developed computer program under LabVIEW™ software environment.

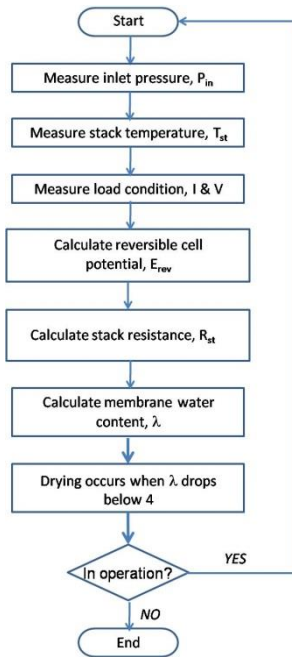


Fig. 1. Algorithm for the prediction of drying.

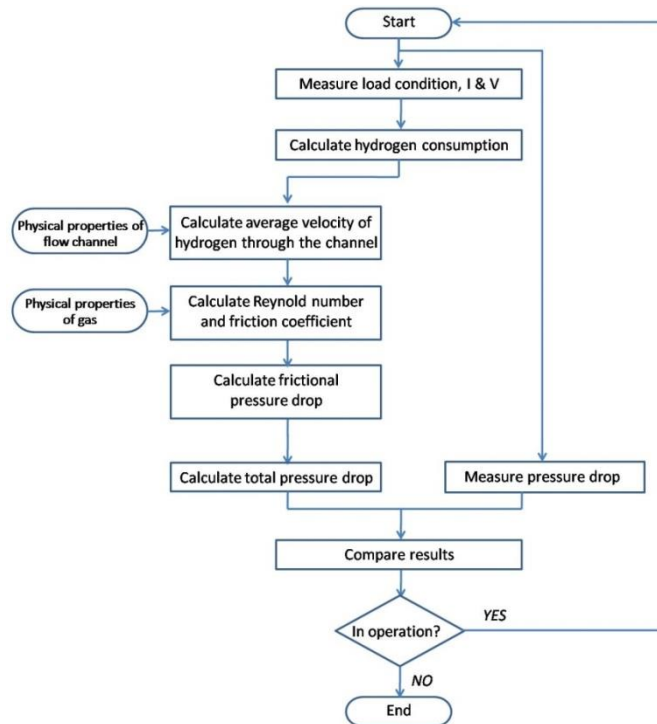


Fig. 2. Algorithm for the prediction of flooding.



Fig. 3. 200W PEM fuel cell stack.

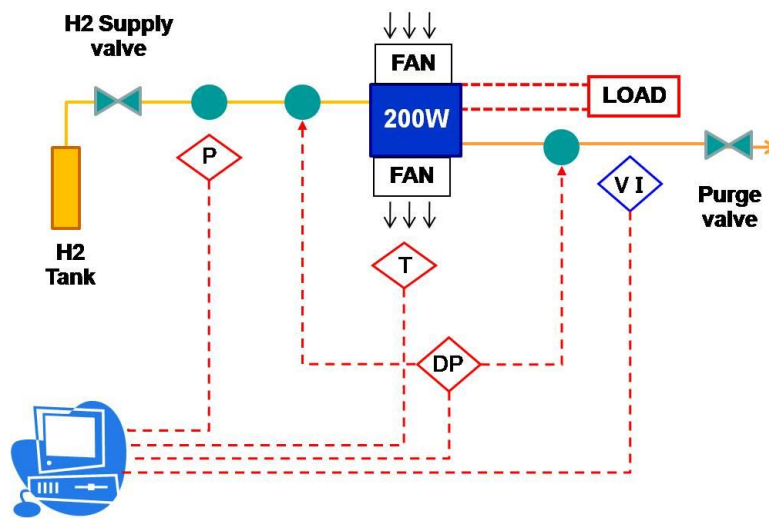


Fig. 4. Measurement diagram of 200W PEM fuel cell stack system.

### 3.2. Monitoring System Development

The main idea of this study is to develop model-based analyzer to compare the real-time measurement of fuel cell's operating conditions with those predicted by the developed model. The fuel cell operating conditions, such as temperature and stack voltage, will be measured using various instruments, such as sensors and electronic load. All measurement data will be the input for developed program under LabVIEW™ environment. Also, the data will be used as inputs to the model. Then, the estimation of the important parameters, which are the resistance and the pressure drop of the cells, was obtained using the fuel cell models. To eliminate the measurement noise, the measurement and monitored signals were fed into arithmetic mean calculation. The model development was mentioned in previous section. The algorithm of the proposed monitoring system is shown in Fig. 5.

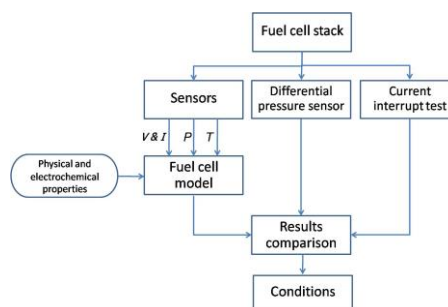


Fig. 5. Structure of the monitoring system.

To validate the model, the system was run and generated sets of data. Then, with the estimated parameters, the model was computed using the generated data. The pressure drop and the resistance of the system were predicted and compared with the available measurement.

### 3.3. The Operating Conditions

An open-cathode fuel cell stack was operated with a constant pressure of 0.45 barg for hydrogen. The cell stack was operated by varying the potential output from high potentials (42.07 V) down to low potentials (24.5 V) for several cycles in order to obtain the polarization curves and find their average value and standard deviation of their corresponding current to represent the cell performance. Then, the cell performance would be used to determine the cell parameters which were exchange current density, transfer coefficient and ohmic resistance. These values represented the values at normal operation which would represent the base case values and would be used for comparing with other operating conditions. To obtain the membrane resistance, the relationship between load current and voltage at various operating conditions was generated by programming the change of the load current into the electronic load. Initially, the fuel cell stack was operated by drawing the current at 2A for 5 minutes. Then, the load current was rapidly decreased to 0A and maintained for 5 minutes. Next, this stepwise current variation of the load current between 2A and 0A was repeated again. Then, the current was risen up to be 3A and finally at 4A. These data were employed to determine the resistances and water contents for these operating conditions.

## 4. Results and Discussion

### 4.1. The Fuel Cell Characteristics

200 W 42-cells fuel cell stack, produced by Horizon Fuel Cell Technologies, was first run in order to collect the relevant data and its performance. Its polarization and power curve were generated as shown in Fig. 6. The open circuit voltage of the stack was 42 volts. The maximum current generated by the stack was 6.42 A, and the maximum power was 172 W at 28 volts. The polarization curve was used for estimating process parameters of the fuel cell.

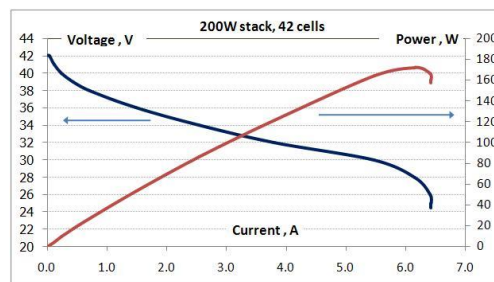


Fig. 6. Fuel cell polarization curve, operating pressure is 0.45 bars.

### 4.2. Estimation of Exchange Current Density and Transfer Coefficient

The steady performance of the PEM fuel cell stack was investigated by measuring the load current for various current and potentials between 5.8 A or 24.5V and 0.05 A or 41 V. As shown in Fig. 7, the output voltage drop could be classified into 3 regions. For the first region where the current density is low, the voltage loss is mainly due to activation loss or due to the kinetics of the electrochemical reaction. Secondly, the output voltage linearly decreases with the increase of the current density. This is due to the resistances in the system which are electrolyte and electronic resistances. Finally, the output voltage dramatically decreases at high current density. This is due to the limitation to supply the reactants for the reaction. The phenomena can be represented by Eqs. (2), (3), and (4). Since the voltage and the current density could be obtained experimentally. The related parameters shown in the equation could be estimated.

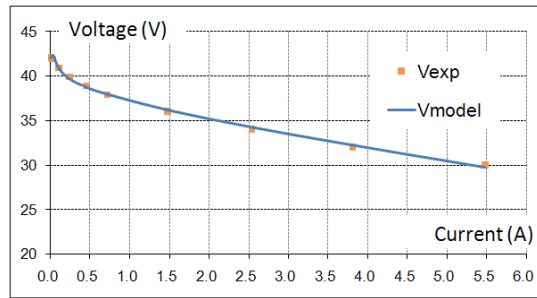


Fig. 7. Polarization curve of 200W PEM fuel cell stack (■ experimental data – curve fitting).

The exchange current density,  $i_0$ , and Tafel slope,  $RT/\alpha F$ , in Eq. (3) were assumed to be independent of the stack temperature. PEM fuel cell also suffers slightly from mass transport loss at the mid-current range. Thus, they are assumed to be constant values. According to the assumptions, data from polarization curve was used to estimate the values of the exchange current density and Tafel slope. Then, the output voltages and the current densities were employed to fit with the parameters in the Eq. (2) when substituting with Eqs. (3) and (4). The parameter estimations were conducted by least square method and the results of the estimations are shown in Table 1. These estimated parameters were used to predict the fuel cell stack voltage ( $V_{model}$ ) at various current densities. Then, they were plotted against the experimental values as shown in Fig. 7. The model was well representing the experimental data and can be used for predicting the cell performance in the subsequent sections.

Table 1. Steady performance fitting parameters.

Run	$i_0$ (mA/cm <sup>2</sup> )	Tafel coefficient, $\frac{RT}{\alpha F}$
1	0.00264	0.0232
2	0.00337	0.0232
3	0.00373	0.0222
4	0.00314	0.0218
5	0.00383	0.0214
6	0.00348	0.0213
7	0.00348	0.0214
Average	0.00338	0.0221
Standard deviation	0.0004	0.0008

### 4.3. Membrane Resistance Estimation

The membrane resistance is a function of stack voltage and load current. To obtain the resistance, the relationship between load current and voltage was generated by programming the change of the load current into the electronic load as mentioned in previous section and shown in Fig. 8. The corresponding voltage responses, obtained corresponding to these operations, were plotted as shown in Figs. 9 and 10.

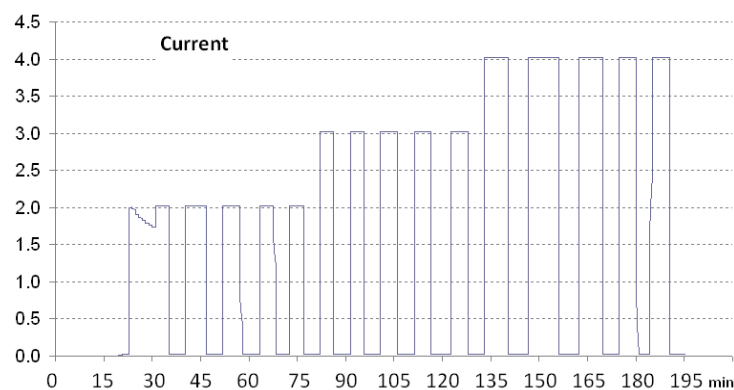


Fig. 8. The prescribed load current schedules between 2 and 4 A.

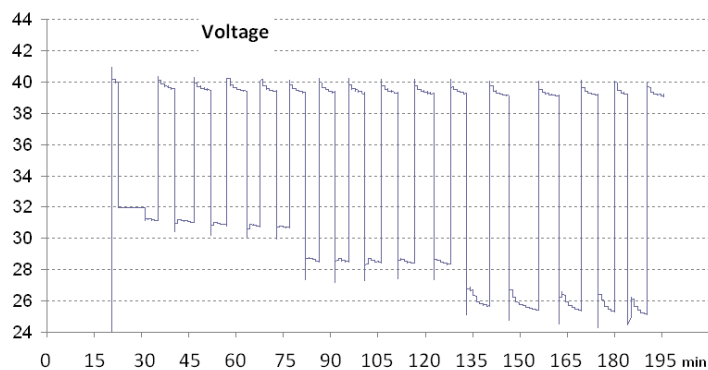


Fig. 9. The measured histories of the output voltage when load current schedules between 2 and 4 A.

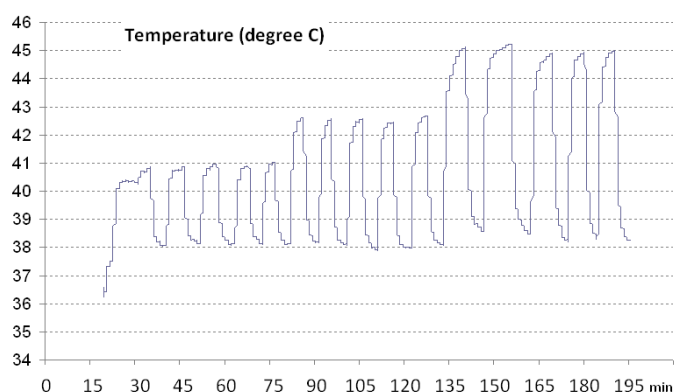


Fig. 10. The measured histories of the stack temperature when load current schedules between 2 and 4 A.

Figure 9 shows the profile of the output voltage obtained during the load current changes as shown in Fig. 8. The output voltage was observed to decrease to a steady-state low value when the load current increased to the high value. On the contrary, the output voltage increased to a steady-state high value when the load current was changed to the open circuit voltage mode. Figure 10 shows the stack temperature gradually evolving upon the load current change. The stack temperature changing during the operation, in turn, influences the theoretical cell voltage ( $E_s, T, P$ ). The measured values of voltage and current from the fuel cell stack were used to estimate the resistance of the fuel cell stack, as results shown in Fig. 11. It should be noted that this procedure should be applied only when the fuel cell operates in the linear region, or ohmic resistance dominating the total potential loss, which is the desired regime for the fuel cell operation. Since the resistance could typically be calculated by dividing the potential change with the current flow. This estimation method would lead to unreliable results when the current flow is close to zero value or when the current flow operates in mass transfer limitation region. According to above discussion, the characteristics of the membrane resistance were investigated only when the current is not zero. The resistance of the membrane, as shown in Fig. 11, is continuously changing due to load current variation which is the function of stack's voltage and temperature. The membrane resistance was found to slightly decrease from 0.95 to 0.7  $\Omega$  as current increased from 2A to 4A.

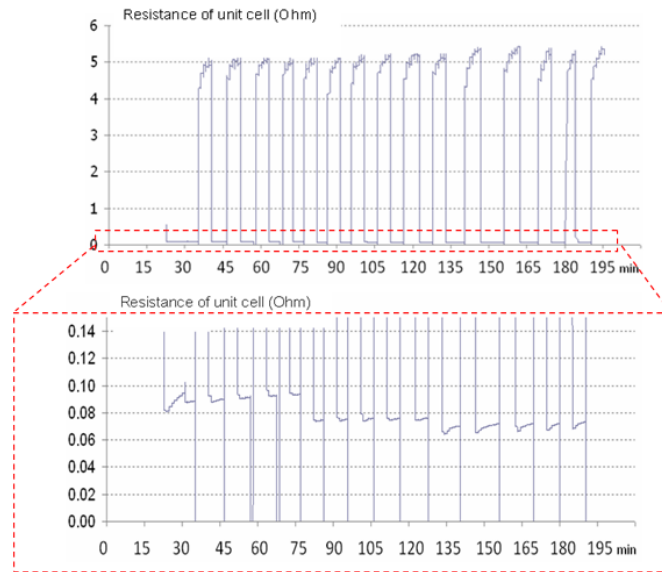


Fig. 11. Predicted resistance of unit cell during current load change operation and its magnification for the small resistance values when load current schedules between 2 and 4 A.

After the membrane resistances were calculated, the water content could be estimated by using Eq. (5). Figure 12 shows the estimate of the membrane water content obtained from the algorithm against the step load current. As can be seen, the estimated membrane water content was initially around 13 to 13.5 mol  $\text{H}_2\text{O}/\text{mol SO}_3\text{H}$  at the load current of 2A. When the current was not drawn from the stack, the cell potential and cell resistance were high. There was no water generated during operation. Thus, the water content in the membrane will be low. Figure 12 estimates the water content to be less than 2 when the cell was running near the open circuit mode. Figure 12 also shows that the estimated values of membrane water content was higher from 13 to 15.5 when the cell was operated at higher load current from 2A to 4A. Using the estimated membrane resistance, as shown in Fig. 11 and the estimated membrane water content, as shown in Fig. 12, it is clear that membrane drying-out has not occurred during the operation of the stack since the water content during these operation was varied between 12 and 16 mol  $\text{H}_2\text{O}/\text{mol SO}_3\text{H}$  [13]. It should be noted that the membrane will dry if water content of the membrane drop below 4. Moreover, the estimated membrane water content seems to be reliable because its value should not be exceeding 22 mol  $\text{H}_2\text{O}/\text{mol SO}_3\text{H}$  [13]. Therefore, the fuel cell drying-out can be identified by monitoring the estimate of the membrane water content.

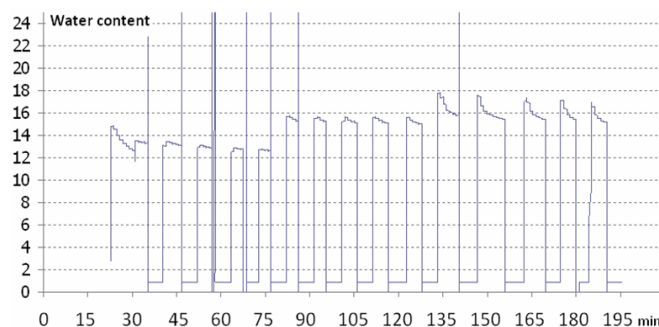


Fig. 12. Predicted membrane water content when load current schedules between 2 and 4 A.

#### 4.4. Monitoring of Fuel Cell Flooding

Flooding is one of the challenging problems for developing a PEM fuel cell. In order to detect flooding condition inside the cell, in the study, the differential pressure sensor was installed to measure pressure difference between the inlet and outlet pressures of the fuel cell stack system. Moreover, load current, temperature, and cell potential were fed into the developed model to estimate the pressure drop across the fuel cell. These two values were compared. The discrepancy between the measured and the estimated

pressure drops indicates the abnormal condition in the fuel cell. Due to the stack limitation, the proposed system for flooding detection was carried out on the anode side by varying the degree of humidification of hydrogen feed.

To validate the developed model for estimating pressure drop across the stack, the fuel cell stack was operated by changing the cell potentials and measuring the corresponding current as shown in Figs. 13-14. These values were measured and sent to the data acquisition system. Then, using Eq. (7-16), they were employed to calculate hydrogen feed rate, friction loss, and pressure drop across the stack, respectively. The calculated values were then plotted against the measured values as shown in Fig. 15. It could be observed that when the fuel cell stack was under load, the predicted pressure drop values were in good agreement with the measured values. Thus, the model also confirms to be used as system representative. Figure 15 also shows a number of spikes pressure drop values along the operation. These spikes were taken place due to the opening and closing of the purge valve in the system in order to maintain the hydrogen concentration in the system and it causes the pressure change abruptly.

Later on to demonstrate the effect of water in the stack, the hydrogen feed was passed through a humidifier to bring in some water into the stack with the hydrogen feed. Using membrane tube inside a humidifier, the inlet hydrogen was humidified at 50°C. Figure 16 shows both of measured and predicted pressure drops when humidified hydrogen was fed. One can observe that the measured pressure drop was higher than the predicted values due to water taking up some space of the gas channel. The spikes on the measured values were also the effect of the opening and closing of the purge valve. Figure 16 shows significant difference between the measured and the predicted values. Thus, the flooding could be identified by tracking the differences. By monitoring the difference, when the pressure difference exceeds the preset value, the system could identify the flooding and the system could take some measures to correct the problem, such as opening the purge valve more frequently to remove water from the channel, or bypassing the hydrogen feed from the humidifier.

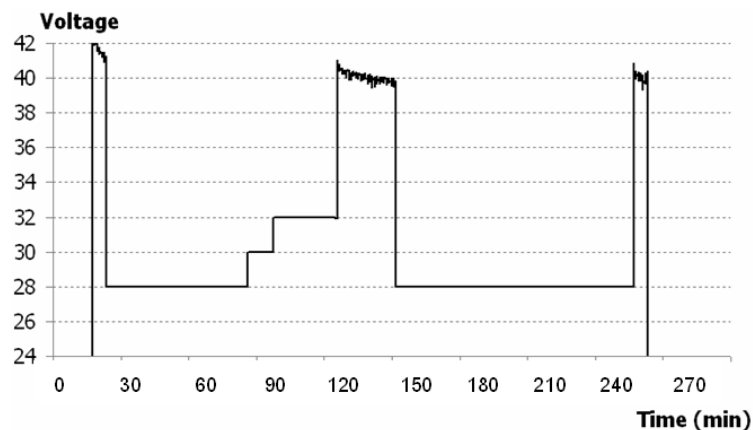


Fig. 13. The prescribed voltage schedules for the pressure drop model validation.

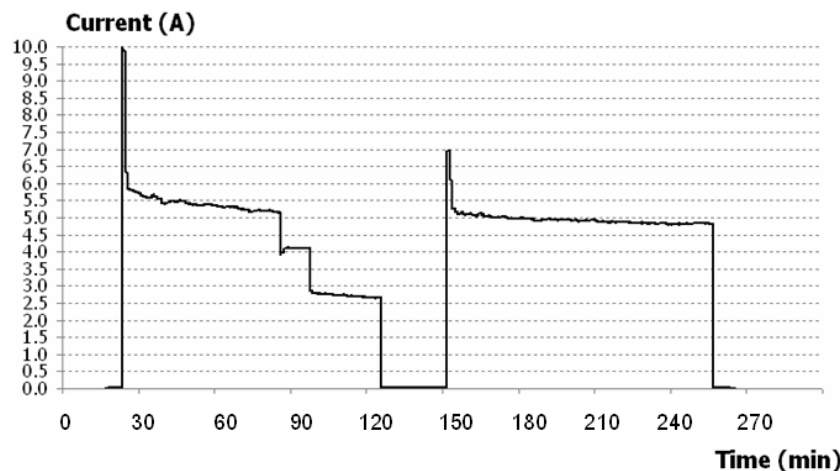


Fig. 14. The response load current for the pressure drop model validation.

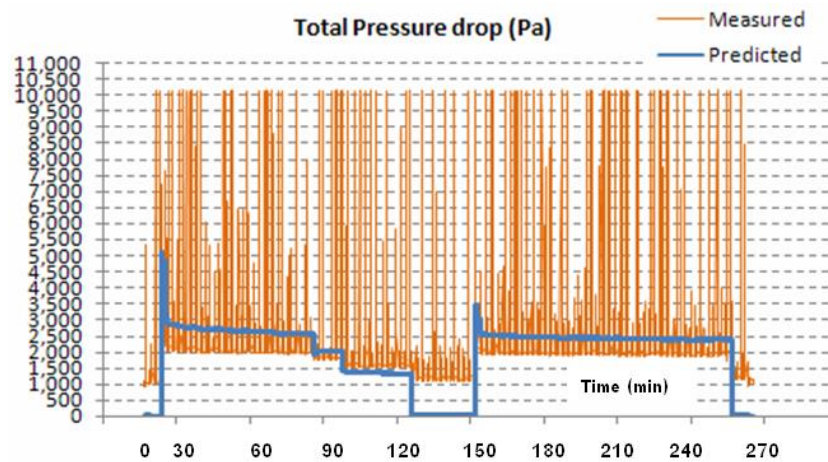


Fig. 15. Comparison of estimated pressure drop and its measured values during normal operation of fuel cell stack.

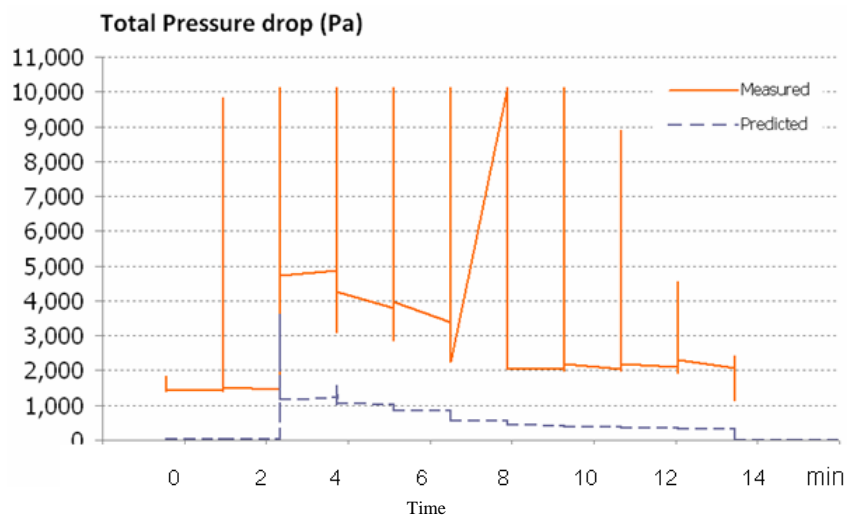


Fig. 16. Comparison of estimated pressure drop and its measured values during fault condition with flooding of fuel cell stack.

## 5. Conclusion

This paper is to develop an online model-based monitoring system for a 200 W PEM fuel cell stack. A number of necessary sensors were installed and transmitted the process variables to the models developed under Labview environment. The model employed the measuring data from the experiment to estimate important process parameters, such as exchange current density, Tafel slope, membrane resistance, and pressure drop in the gas channels. The drying-out of the fuel cell could be observed from the membrane resistance, while flooding conditions could be detected from the increase of the pressure drop inside the gas flow field. Thus, the study had demonstrated that the developed model could be used to identify those phenomena by monitoring the water content estimate using the discrepancy between the measured and predicted pressure drops.

## Acknowledgements

This work was supported by the Higher Education Research Promotion and National Research University of Thailand, Office of the Higher Education Commission (EN276B), by Center of Excellence on Petrochemical and Materials Technology, Chulalongkorn University and by Graduate School Chulalongkorn University.

## References

- [1] J. Laminie and A. Dicks, *Fuel Cell Systems Explained*. USA: John Wiley & Sons, 2003.
- [2] F. Barbir, *PEM Fuel Cells: Theory and Practice*. USA: Elsevier Academic Press, 2005.
- [3] F. Barbir, H. Görgün, and X. Wang, "Relationship between pressure drop and cell resistance as a diagnostic tool for PEM fuel cells," *J. Power Sources*, vol. 141, pp. 96–101, 2005.
- [4] P. Pei, M. Ouyang, W. Fang, L. Lu, H. Haung, and J. Zhang, "Hydrogen pressure drop characteristic in a fuel cell stack," *Int. J. Hydrogen Energ.*, vol. 31, pp. 371–377, 2006.
- [5] J. Stumper, M. Löhr, and S. Hamada, "Diagnostic tools for liquid water in PEM fuel cells," *J. Power Sources*, vol. 143, pp. 150–157, 2005.
- [6] J. Kim, S. M. Lee, S. Srinivasan, and C. E. Chamberlin, "Modeling of proton exchange membrane fuel cell performance with an empirical equation," *J. Electrochem. Soc.*, vol. 142, no. 8, pp. 2670–2674, 1995.
- [7] H. Görgün, M. Arcak, and F. Barbir, "An algorithm for estimation of membrane water content in PEM fuel cells," *J. Power Sources*, vol. 157, pp. 389–394, 2006.
- [8] H. P. Ma, H. M. Zhang, J. Hu, Y. H. Cai, and B. L. Yi, "Diagnostic tool to detect liquid water removal in the cathode channels of proton exchange membrane fuel cells," *J. Power Sources*, vol. 162, pp. 469–473, 2006.
- [9] X. Liu, H. Guo, F. Ye, and C. F. Ma, "Water flooding and pressure drop characteristics in flow channels of proton exchange membrane fuel cells," *Electrochim. Acta*, vol. 52, pp. 3607–3614, 2007.
- [10] J. Chen and B. Zhou, "Diagnostic of PEM fuel cell stack dynamic behaviors," *J. Power Sources*, vol. 177, pp. 83–95, 2008.
- [11] S. K. Roy and M. E. Orazem, "Analysis of flooding as a stochastic process in polymer electrolyte membrane (PEM) fuel cells by impedance techniques," *J. Power Sources*, vol. 184, pp. 212–219, 2008.
- [12] M. A. Danzer and E. P. Hofer, "Electrochemical parameter identification—An efficient method for fuel cell impedance characterization," *J. Power Sources*, vol. 183, pp. 55–61, 2008.
- [13] N. Fouquet, C. Doulet, C. Nouillant, G. Dauphin-Tanguy, and B. Ould-Bouarnama, "Model-based PEM fuel cell state-of-health monitoring via ac impedance measurements," *J. Power Sources*, vol. 159, pp. 905–913, 2006.
- [14] X. Xue, J. Tang, N. Sammes, and Y. Ding, "Model-based condition monitoring of PEM fuel cell using Hotelling  $T^2$  control limit," *J. Power Sources*, vol. 162, pp. 388–399, 2006.
- [15] L. A. M. Riascos, M. G. Simoes, and P. E. Miyagi, "On-line fault diagnostic system for proton exchange membrane fuel cells," *J. Power Sources*, vol. 175, pp. 419–429, 2008.
- [16] G. Mulder, F. D. Ridder, P. Conen, D. Weyen, and A. Martens, "Evaluation of an on-site cell voltage monitor for fuel cell systems," *Int. J. Hydrogen Energ.*, vol. 33, pp. 5728–5737, 2008.
- [17] D. Gerteisen, T. Heilmann, and C. Ziegler, "Modeling the phenomena of dehydration and flooding of a polymer electrolyte membrane fuel cell," *J. Power Sources*, vol. 187, pp. 165–181, 2009.
- [18] Y. Mugikura and K. Asano, "Analysis of polymer electrolyte fuel cell performance by electrode polarization model," *J. Power Sources*, vol. 193, pp. 32–38, 2009.
- [19] T. E. Springer, T. A. Zawodzinski, and S. Gottesfeld, "Polymer electrolyte fuel cell model," *J. Electrochem. Soc.*, vol. 138, pp. 2334–2342, 1991.
- [20] X. Yu, M. Pingwen, H. Ming, Y. Baolian, and Z. G. Shao, "The critical pressure drop for the purge process in the anode of a fuel cell," *J. Power Sources*, vol. 175, pp. 163–169, 2008.
- [21] F. Barbir, H. Gorgun, and X. Wang, "Relationship between pressure drop and cell resistance as a diagnostic tool for PEM fuel cells," *J. Power Sources*, vol. 141, no. 1, pp. 96–101, 2005.
- [22] T. A. Zawodzinski, "Membranes performance and evaluation," presented at *NSF Workshop on Engineering Fundamentals of Low-Temperature PEM Fuel Cells*, Arlington, VA, November 2001.